THE JOURNAL OF PHYSICAL CHEMISTRY A

ARTICLE

pubs.acs.org/JPCA

Water Dynamics at Protein Interfaces: Ultrafast Optical Kerr Effect Study

Kamila Mazur, Ismael A. Heisler, and Stephen R. Meech*

School of Chemistry, University of East Anglia, Norwich NR4 7TJ, U.K.

ABSTRACT: The behavior of water molecules surrounding a protein can have an important bearing on its structure and function. Consequently, a great deal of attention has been focused on changes in the relaxation dynamics of water when it is bound at the protein surface. Here we use the ultrafast optical Kerr effect to study the H-bond structure and dynamics of aqueous solutions of proteins. Measurements are made for three proteins as a function of concentration. We find that the water dynamics in the first solvation layer of the proteins are slowed by up to a factor of 8 in comparison to those in bulk water. The most marked slowdown was observed for the most hydrophilic protein studied, bovine serum albumin, whereas the most hydrophobic protein, trypsin, had a slightly smaller effect. The terahertz Raman spectra of these protein solutions resemble those of pure water up to a concentration of 5 wt %, above which a new feature appears at ~80 cm^{-1}, which is assigned to a bending of the protein amide chain.

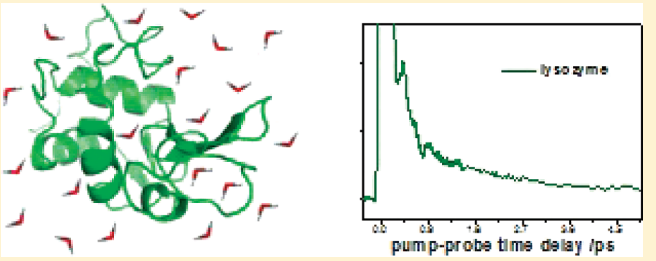

INTRODUCTION

The waters of solvation surrounding biomolecules control many important biological processes. For example, they play a crucial role in the folding and function of proteins and enzymes, whereas the structure and conformation of DNA depends on the hydration water.[1,2] Therefore, the understanding of water at these interfaces is of great importance in chemistry and biology.[3−7]

Water molecules in aqueous solutions of proteins can be grouped into three broad categories: (1) the internal waters that occupy specific sites in the protein and can be identified crystallographically, (2) the hydration water immediately surrounding the protein, and (3) bulklike water. Hydration water has direct contact with the protein surface and plays an essential role in protein folding interaction of water with the hydrophobic groups, causing them to collapse and become isolated in the protein core. Thus the protein core contains more than 80% of the hydrophobic side chains.[8] The water molecules that solvate the external surface of a protein are also functionally significant; it is known that to fully activate the dynamics and functionality of a protein, 0.40 g of water per gram of protein is required.[9] Because of this importance the hydration layers surrounding peptides,[10−12] proteins,[7,13,14] and carbohydrates[15] have been the subject of a large number of studies in recent years. It is established that the dynamics of hydration water are distinct from those of bulk water;[16] however, the nature and extent of these differences are still a matter of debate.[7] Molecular dynamics (MD) simulations[17] and NMR studies[18] showed that the H-bonds between protein and water are preferentially formed where water hydrogen atoms act as donors, with the number of H-bonds depending strongly on the polar character of the protein surface. MD simulations have shown that the rearrangement of the protein hydration network occurs at subpicosecond to picosecond time scales.[4] This view was consistent with NMR data that found a highly mobile protein solvation layer, retarded by no more than a factor of 2 compared to that of the bulk.[13] Single frequency terahertz transmission spectroscopy has also been applied to the study of hydration water of peptides[12] and proteins.[19,20] This approach suggested that a dynamical solvation layer could extend considerably beyond the monolayer suggested by static experiments. It was suggested that this method was also more sensitive to the effect of folded state of the protein on solvation structure.

In this work we employ the optically heterodyne detected optical Kerr effect (OHD-OKE) method to probe dynamics in the aqueous solvation shell of proteins over a wide concentration range. OHD-OKE has been proven as a sensitive probe of the dynamics of molecular liquids[21,22] and complex fluids,[23,24] and has recently been applied to study dynamics of aqueous solutions,[25−28] including peptides and proteins.[11,29,30] The OHD-OKE has two advantages for the study of aqueous solvation dynamics. First, it measures solution dynamics in real time, in contrast to dielectric relaxation, scattering methods and NMR methods, in which the picosecond dynamics must be indirectly inferred. Second, the OHD-OKE reveals the terahertz Raman spectral density, which, for aqueous solutions in particular, reflects changes in the H-bonded structure of water brought about by the solute.[28,31]

Special Issue: Femto10: The Madrid Conference on Femtochemistry

Received: August 4, 2011
Revised: September 19, 2011

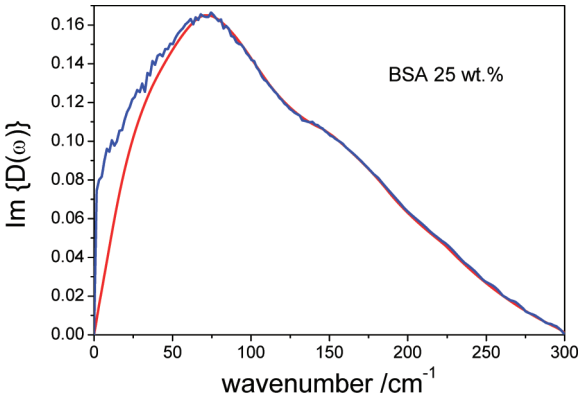

Figure 1. Complete Im $D(\omega)$ (blue) and reduced Im $D'(\omega)$ (red) Raman spectral densities for a 25 wt % solution of BSA.

EXPERIMENTAL SECTION

OHD-OKE is a time-resolved nonresonant nonlinear optical method in which relaxation of the transient polarizability anisotropy induced by an ultrafast linearly polarized pump pulse is measured. The laser source used here was a home-built titanium sapphire laser with 250 mW output power and a repetition rate of 68 MHz. The pulses were of 42 fs duration, centered at a wavelength 815 nm. A conventional OHD-OKE geometry was employed.[32] The detected signal, $S(t)$, is a convolution of solution polarizability response function, $R(t)$ with the instrument response function, $G^{(2)}(t)$, which is the second-order autocorrelation of the laser pulses, $S(t) = R(t) \otimes G^{(2)}(t)$. Both single molecule and interaction-induced processes and their cross terms contribute to the observed signal. Further details of OHD-OKE spectroscopy can be found elsewhere.[32,33]

The signal $S(t)$ can generally be separated into fast (subpicosecond) and slow (picosecond to nanosecond) contributions. The former typically manifests oscillatory behavior and contains information about nondiffusive and interaction-induced dynamics, and the latter exhibits monotonic, often non-single-exponential relaxation and contains information on diffusive orientational relaxation and H-bond network reorganization.[34]

The dynamics acquired through OHD-OKE can be analyzed in both time and frequency domain. The frequency domain representation is readily calculated from the Fourier transform deconvolution relationship:[32]

$$\frac{\mathrm{FT}[S(t)]}{\mathrm{FT}[G^{(2)}(t)]} = D(\omega)$$

The imaginary (Im) part of $D(\omega)$ contains only information about the nuclear part of the polarizability anisotropy response.[32] The result is the Raman spectral density (RSD), Im $D(\omega)$. To highlight the fast (higher frequency) dynamics, the picosecond response can first be subtracted from $S(t)$ to yield the reduced RSD Im $D'(\omega)$. In Figure 1 an example of the two RSDs are shown.

Samples. Lysozyme from chicken egg white (molecular weight 14.3 kDa), trypsin from bovine pancreas (molecular weight 23.8 kDa), and albumin from bovine serum (BSA, molecular weight. 66 kDa) were purchased from Sigma Aldrich. All samples were used as received. Aqueous solutions were prepared with concentrations between 0 wt % up to the maximum possible concentrations of 15, 25, and 30 wt % for trypsin, BSA, and lysozyme, respectively. To remove any undissolved matter, all samples were filtered through a 0.22 μm Millipore filter.

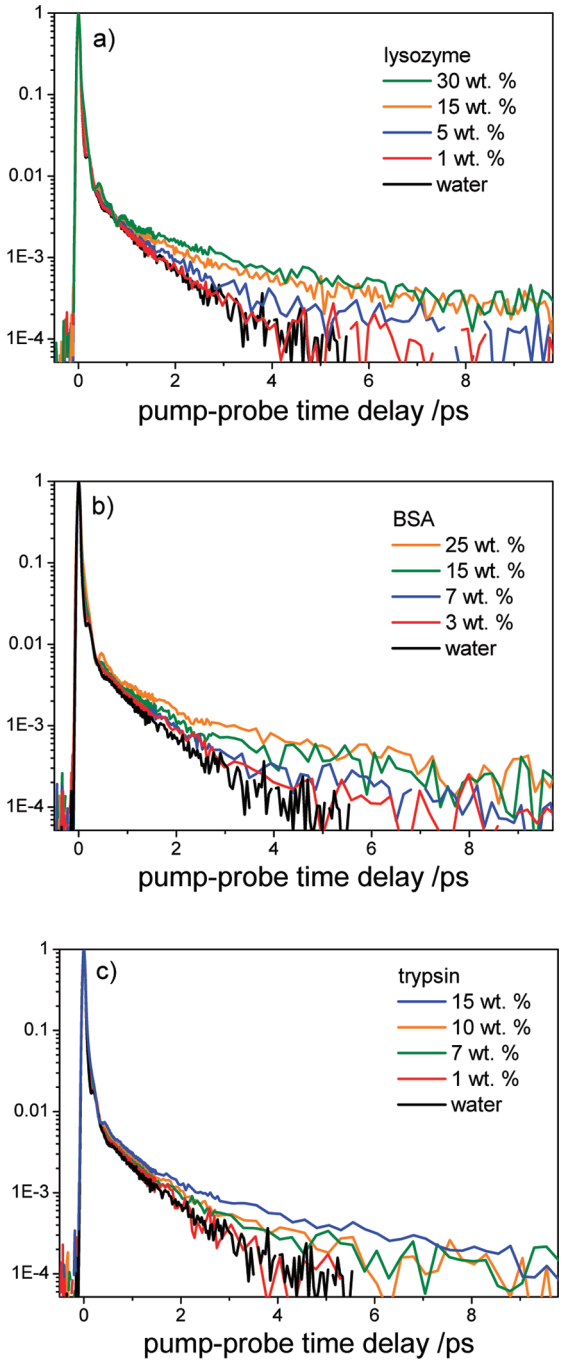

Figure 2. OKE−OHD signals for three proteins as a function of wt % (a) lysozyme, (b) BSA, and (c) trypsin. Water is plotted in black for reference.

Viscosity. Viscosity measurements were carried out using an Ostwald type viscometer, with the viscometer constant 0.010 9. Each measurement was repeated three times, in the temperature range 19 ± 1 °C, and an average was taken.

RESULTS AND DISCUSSION

Picosecond Relaxation Time. The dynamics of pure water have been the subject of extensive studies in recent years by

dx.doi.org/10.1021/jp2074539 |J. Phys. Chem. A XXXX, XXX, 000–000

means of several different spectroscopic techniques.[31,35−39] The water time domain data recovered from the OHD-OKE are shown in black in Figure 2. The peak at $t = 0$ arises from the instantaneous electronic response and does not contain any information about the molecular structural dynamics; it is removed in the FT analysis described above. In the subpicosecond (or terahertz) spectral region the water spectrum is characterized by three modes, all of which arise mainly from interaction induced relaxation rather than molecular reorientation. This is a consequence of the near isotropic polarizability of water.[40] A shoulder at 200 fs corresponds to a ∼50 cm^{-1} band in the terahertz spectrum and is typically (though not unambiguously—see below) associated with an intermolecular H-bond bending mode.[37,41,42] An oscillatory feature near 50 fs is the origin of a mode at ∼175 cm^{-1}, which is assigned, on the basis of MD calculations, to an intermolecular H-bond stretching vibration.[42,43] On an even faster time scale a third broad band, observed in a spectral region above ∼400 cm^{-1}, originates from librational dynamics and was not fully resolved with our present time resolution.[44]

The water relaxation dynamics beyond 1 ps are characterized by a non-single-exponential relaxation function and result from translational and rotational−translational dynamics of water molecules within the H-bonded network.[44] The mean relaxation time is about 800 fs, which is on the same order of magnitude as the observed rotational reorientation time for bulk water, but somewhat faster than it. Laage and Hynes[45] recently described an extended molecular jump mechanism for water reorientation in which rotational and translational motions are strongly coupled. In this model, the reorienting water OH group forms an H-bond with another water molecule. When a new water molecule arrives, this H-bond elongates and at the transition state forms a symmetric bifurcated H-bond with two water molecules. The initial H-bond breaks, and a new H-bond with a second water molecule is stabilized. It is plausible that the translational and H-bond dynamics accompanying this orientational jump are reflected in the picosecond polarizability relaxation. A more definite assignment may be possible with improved MD simulations of the water polarizability relaxation.

The OKE responses of aqueous solutions of lysozyme, trypsin, and BSA were studied over a wide range of concentrations, from 0 wt % to their solubility limit. The time domain data are shown in Figure 2. It is evident that for all solutions studied the picosecond relaxation dynamics become slower with increasing concentration, and the departure from single exponential relaxation becomes more marked compared to that of pure water.

The time domain data were fitted to the biexponential decaying function:

$$[1 - \exp(-t/t_r)][a_1 \exp(-t/\tau_1) + a_2 \exp(-t/\tau_2)]$$

where a_i denotes amplitude and t_r is a fast rise time. The exact value of the rise time (typically a few tens of femtoseconds) does not influence the results. During the measurement it was observed that the signal for the solutions with a high concentration of protein did not return to the baseline after 20 ps. In cases where protein concentration exceeded 7 wt %, a small offset (0.000 05) was included to account for this to give a better quality fit. The origin of this offset was not investigated further but may reflect a slow relaxation associated with the protein solute, because at these higher concentrations protein modes also contribute to the RSD (see below).

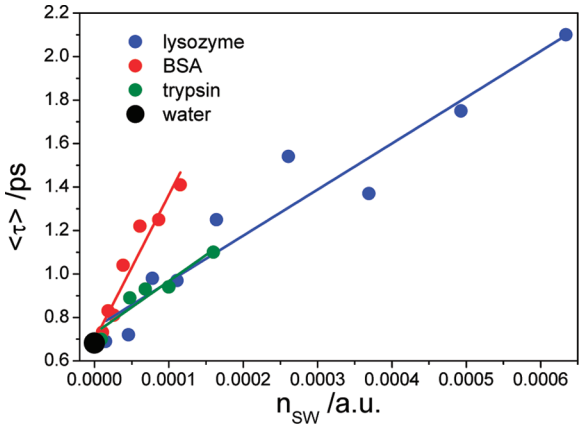

Figure 3. Average relaxation time plotted against molar ratio. Solid lines are linear fits to the data.

The lifetimes and weights obtained from the fit to above equation were used to calculate the averaged relaxation time from the relation:

$$\langle\tau\rangle = \frac{a_1}{a_1 + a_2}\tau_1 + \frac{a_2}{a_1 + a_2}\tau_2$$

The average relaxation times are plotted as a function of the molar ratio, n_{SW} (moles of solute divided by moles of water) in Figure 3.

At the concentrations studied it is unlikely that the protein itself contributes anything other than the constant offset described above to the relaxation times observed. The rotational correlation time of lysozyme and BSA obtained through NMR are 18 and 105 ns, respectively.[46] These values are on a much longer time scale than that probed in the present OHD-OKE experiments. Therefore, we assign the observed concentration dependence of the mean relaxation time to the effect of the protein solute on the dynamics in the water solvent. As measurements obtained by the OHD-OKE technique do not allow the separate measurement of hydration water and free water, we employ a model in which the average relaxation time $\langle\tau\rangle$ is represented by a sum of the free water relaxation time, τ_{WF} (obtained from the bulk water measurement) and an unknown hydration water relaxation time, τ_{WH}, weighted by their respective mole fraction, X_i:[15]

$$\langle\tau\rangle = X_{WF}\tau_{WF} + X_{WH}\tau_{WH}$$

For the protein solutions studied, even at the highest concentration of 30 wt %, it was calculated (see below) that there are at least two hydration shells available for each protein. For such dilute samples the above equation can be rewritten as

$$\langle\tau\rangle = n_{SW}n_m(\tau_{WH} - \tau_{WF}) + \tau_{WF}$$

where n_{SW} is the molar ratio and n_m is the number of water molecules in the first hydration shell. The slopes obtained by fitting the data (Figure 3) to a linear function yield $n_m(\tau_{WH} - \tau_{WF})$. Knowing that the proteins studied have roughly spherical shapes (globular proteins), the volumes could be calculated using the radii 15.9, 18.7, and 27.1 Å for lysozyme, trypsin, and BSA, respectively.[47] With this information, the number of water molecules in each hydration shell could be calculated.[28] For the first hydration shell, the n_m values obtained were 490, 668, and 1385 for lysozyme, trypsin, and BSA, respectively. These

dx.doi.org/10.1021/jp2074539 |J. Phys. Chem. A XXXX, XXX, 000–000

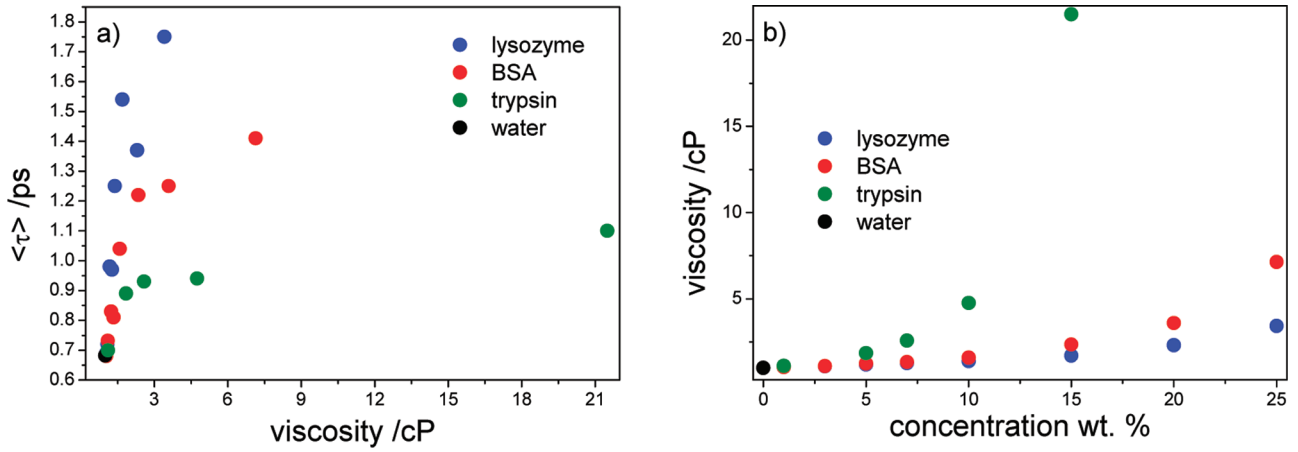

Figure 4. (a) Dependence of average relaxation time on the solution viscosity. (b) Dependence of viscosity on the concentration.

values are in good agreement with published data: 436−644 for lysozyme[48−50] and 1422 for BSA.[51] Using the calculated n_m data and the slope, $n_m(\tau_{WH} - \tau_{WF})$, the hydration water relaxation times were estimated.

First, under the assumption that only water dynamics in the first hydration shell are affected by the protein molecules, we estimated the hydration water relaxation times to be 5.5, 5, and 4.1 ps for BSA, lysozyme, and trypsin, respectively. As the relaxation of pure water is ∼0.7 ps, the estimated relaxation times correspond to factors of 8.0 (BSA), 7.3 (lysozyme), and 6.1 (±0.3) (trypsin) times slower than for bulk water. The retardation factor for the reorientational dynamics of water in the protein hydration shells was studied previously.[3,13,48] For example, from magnetic relaxation dispersion[13] studies the water retardation factor was found to be 2; from depolarized light scattering[3] measurements it was suggested to vary between 6 and 7. Although OHD-OKE accesses translational dynamics, the retardation factor of ∼7 is comparable with these results, though clearly longer than the magnetic relaxation data. This similarity may indicate that translational and reorientational dynamics are correlated, perhaps because both are dominated by the dynamics of water H-bonded network. This correlation is supported by MD simulations of solvated lysozyme[48] where it was found that the rotational relaxation of water at the protein surface presents the same retardation value as does translational diffusion. This factor was calculated to be 3−7 times slower than in the bulk, with the ratio depending on how the hydration shell was defined prior to calculations.

Previously we found similar retardation factors in the OKE relaxation for aqueous solutions of small solutes[28] (e.g., urea and tetamethylurea). This indicates that the slowing down of water dynamics does not depend markedly on the size of the solute, as already concluded from NMR.[14,52] By studying aqueous solutions of peptides through OHD-OKE, we previously found retardation factors varying between 12 and 20.[11] This rather large retardation may indicate that peptides influence the water dynamics beyond the first hydration shell, as only the first hydration shell was taken into account to estimate these relaxation times. Alternatively, the flexibility of the peptide molecule may have contributed to the observed OKE relaxation time, an alternative that will be resolved by study of different peptides. However, the linearity of the plots in Figure 3 is consistent with a negligible protein concentration to the present picosecond time scale relaxation.

Next we try to connect the observed relaxation times with the surface hydrophobicity of the proteins. Protein hydrophobicity was extensively studied in the past using a number of approaches, including hydrophobic interaction chromatography,[53,54] fluorescence spectroscopy,[55] and osmotic pressure measurements.[56] Lee and Richards[57] estimated surface hydrophobicity of lysozyme from numerical calculations of the solvent accessible area. They found that lysozyme has an approximately 41% hydrophobic surface. The surface of BSA, studied through both osmotic pressure measurements and hydrophobic interaction chromatography,[56] was found to be significantly more hydrophilic than the one of lysozyme. Wettability and contact angle analysis[58] of lysozyme and trypsin films indicated trypsin as the protein with the most hydrophobic surface. Therefore, the surface hydrophobicity of the proteins studied can be written in the order trypsin < lysozyme < BSA, with the BSA being the most hydrophilic.

The effect of hydrophobic sites on the dynamics of solvating water molecules was studied by many groups.[28,59−62] There is, however, incomplete agreement over whether hydrophobic or hydrophilic groups have the greater impact on water dynamics. Bakker et al.[59] and Heyden et al.[60] using mid infrared spectroscopy and terahertz spectroscopy, respectively, concluded that hydrophobic sites influence water dynamics to a greater extent than hydrophilic ones. Quite the opposite was found by means of MD calculations[61] and quasi-elastic neutron scattering.[62] Our previous OKE studies of peptides[11] and small solutes[28] found that hydrophilic groups caused a bigger retardation effect on the dynamics of the hydration shell observed in OKE. In this work we also find the largest retardation factor for the proteins with the most hydrophilic surface (BSA) and the smallest retardation factor for the most hydrophobic (trypsin). This is thus consistent with the hydrophilic interaction having the greatest retardation effect on the dynamics of the solvating water molecules.

A further factor to be considered is the possibility that water dynamics in a second hydration shell are also affected by the protein. If a second shell is included, the calculated retardation factor will be smaller, yielding values of 4.1, 3.5, 3.1 (±0.2) for BSA, lysozyme, and trypsin, respectively. The smaller difference in the retardation factor between different proteins indicates that water relaxation dynamics in the second hydration shell are similar in all proteins studied, regardless of their hydrophobicity. Water molecules in the second hydration shell do not have a

dx.doi.org/10.1021/jp2074539 |J. Phys. Chem. A XXXX, XXX, 000–000

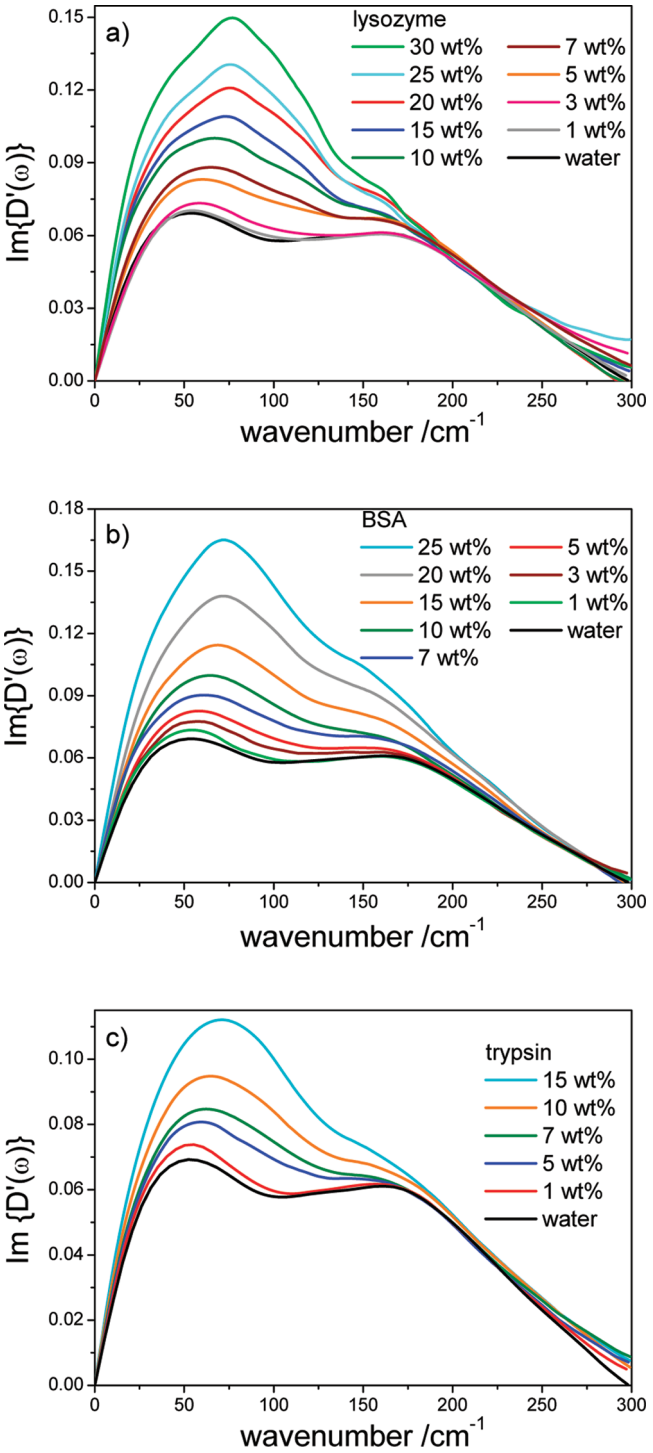

Figure 5. Evolution of RSD spectra of (a) lysozyme, (b) BSA, and (c) trypsin with concentration. Pure water is plotted in black.

direct contact with the protein surface and are therefore not strongly affected by the nature of the surface. From our experiments, however, it is impossible to estimate the distance over which the protein affects the water dynamics in its vicinity.

Finally, we consider the relationship between the macroscopic solution viscosity and the observed picosecond relaxation dynamics. The viscosities of the protein solutions were measured as a function of concentration and the average relaxation time, $\langle\tau\rangle$, is plotted against viscosity (Figure 4a). The viscosity of trypsin was found to be the largest among the proteins studied (Figure 4b); at 15 wt % its viscosity is approximately 9 (12) times higher than for BSA (lysozyme) solutions. However, this large viscosity is not reflected in the relaxation times measured in OHD-OKE, because trypsin in fact has the fastest average relaxation time (Figure 4a). From this data we can conclude that the macroscopic solution viscosity is not correlated with the observed relaxation times. The relaxation times we observe arise from microscopic intermolecular interactions whereas the macroscopic viscosity presumably reflects the slower dynamics in the concentrated protein solutions.

Reduced Spectral Density Spectra. The RSDs of the three proteins at different concentrations are shown in Figure 5. Prior to Fourier transformation all data were normalized to the intensity of the electronic response at $t = 0$ ps. Up to 5 wt % the RSDs closely resemble that for pure water, characterized by two bands at ~45 and ~175 cm^{-1}. As mentioned earlier, these can be related to H-bond bending and stretching modes, respectively, although the role of hydrogen bond in the former is still a matter of debate. It has been proposed that this low frequency band originates from the bend of a central molecule within the cage formed by its neighbors. Nakayama[63] using simple models of low energy excitations in water concluded that the low frequency mode is a strongly localized mode, whereas the 175 cm^{-1} mode can be associated with motion mesoscopically distributed over the H-bonded water network. Consequently, in this work the change in water H-bonding structure will be characterized by the evolution in the ~175 cm^{-1} mode of the water spectrum.

For the purpose of the analysis of spectral line shapes, the RSDs were fitted with a sum of two (<5 wt %) or three (>5 wt %) line shape functions. To fit the lysozyme spectra, two more functions were added at concentrations >10 wt %. The wavenumbers of these two extra components are 108 and 160 cm^{-1} and are constant for the whole range of concentrations. Both modes were previously observed in the Raman spectra,[64] of dry lysozyme crystals (at 114 and 167 cm^{-1}) and were assigned to intramolecular modes. The spectra of BSA with three fitting functions and lysozyme with five fitting functions are shown in Figure 6.

The lowest frequency part of the RSD was fitted with the Bucaro−Litovitz (BL) function:[65]

$$I_{BL} = A_{BL}\omega^{\alpha}\ \exp[-(\omega/\omega_{BL})]$$

where ω_{BL} is a characteristic frequency and α a fitting parameter. The highest frequency part was fitted with an antisymmetrized Gaussian (ASG), which has the form:

$$I_{ASG} = A_{ASG}\left[\exp\left[-\frac{\omega-\omega_{ASG}}{\Delta\omega_{ASG}}\right]^2 - \exp\left[-\frac{\omega+\omega_{ASG}}{\Delta\omega_{ASG}}\right]^2\right]$$

An intermediate frequency component was required for all samples with >5 wt % protein, with the form of a Gaussian (G) line shape:

$$I_G = A_G\ \exp\left[-\frac{\omega-\omega_G}{\Delta\omega_G}\right]^2$$

where in each case A_i denotes the amplitude, ω_{ASG} and ω_G are the central frequencies, and $\Delta\omega_{ASG}$ and $\Delta\omega_G$ are the full widths at half-maximum.

dx.doi.org/10.1021/jp2074539 |J. Phys. Chem. A XXXX, XXX, 000–000

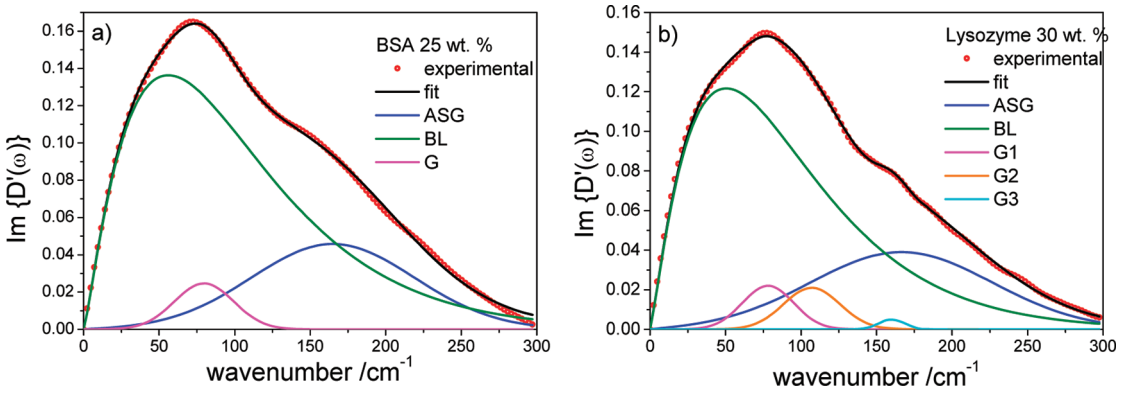

Figure 6. (a) RSD of BSA 25 wt % fitted with three functions: Bucaro−Litovitz (BL), antisymmetrized Gaussian (ASG), and Gaussian (G). The dotted line is the experimental data and black line is a sum of three fitting functions. (b) RSD of lysozyme 30 wt % fitted with five functions.

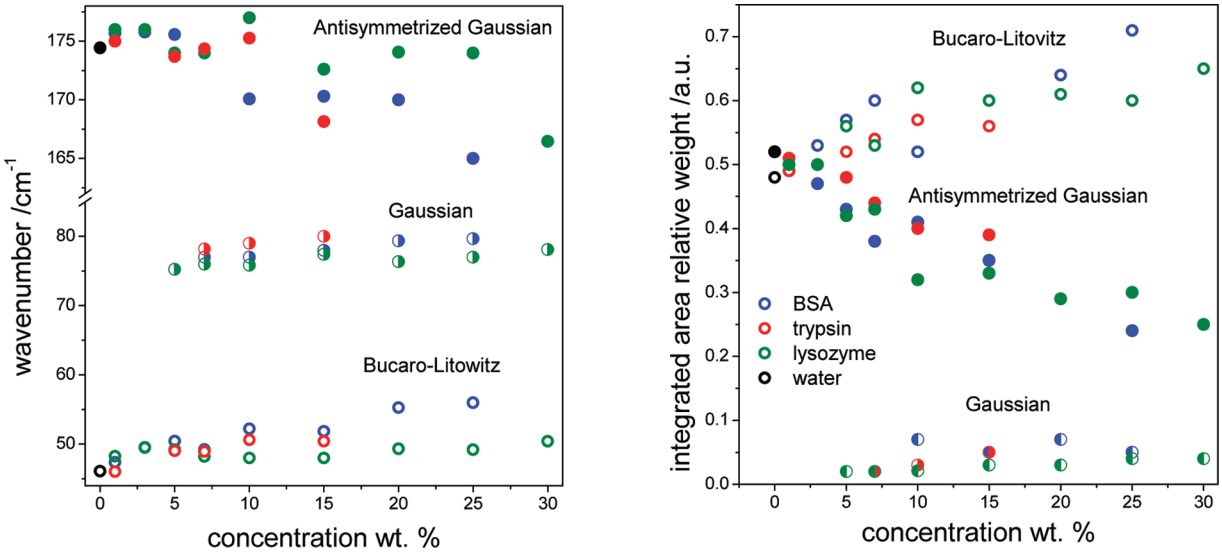

Figure 7. Parameters obtained from the fit of the Bucaro−Litovitz (open symbols), antisymmetrized Gaussian (filled symbols), and Gaussian line shape functions (half filled) to the protein RSD of BSA (blue), trypsin (red), and lysozyme (green), as a function of concentration.

The fitting parameters are shown in Figure 7. The integrated area relative weight was calculated using equations

$$I_i = \frac{I_i}{I_{\mathrm{TOT}}}$$

where i is either BL, ASG, or G and I_{TOT} is the total integrated area of the RSD. There is only a slight shift of the BL mode toward higher frequencies with increasing concentration. However, the fraction of the RSD assigned to BL increases significantly with increasing concentration. The increase in the relative amplitude at higher concentrations may be assigned to a contribution originating from protein modes in this frequency region. Such solute modes were previously observed in formamide[66,67] and *N*-methylacetamide[68] (NMA), which are model compounds for the protein amide backbone. However, some other solutes, for example, sodium iodide, are known cause a shift of the water RSD to lower frequency. The mixture of protein and water bending mode renders assignment of this spectral component complex.

Both the wavenumber and the relative weight of the ASG mode decrease with increasing concentration at >5 wt % protein. In pure water this mode is associated with the collective water−water H-bond stretching motion, so this observation indicates a weakening or disruption of water−water hydrogen bonds by the protein. A weakening of the H-bond might be expected to lead to faster relaxation dynamics, which is not what is observed (Figure 2). Two factors may lead to this result. First, the collective mode disrupted by the solute is replaced by a stronger solute −solvent interaction. Second, Laage and Hynes[69] showed that geometric restrictions may slow water orientational dynamics by restricting the approach of a partner water to allow the H-bond switch and associated extended orientational jump that dominates orientational relaxation in bulk water. Similar geometric arguments may apply to the interaction induced dynamics reported by OKE, giving rise to the slower OHD-OKE response even though the characteristic signature of H-bonding is disrupted. The simulations of Marchi et al.[48] showed that translational and orientational dynamics were equally slowed at the protein interface, consistent with this argument.

The intermediate (G) component, which appears at concentrations above 5 wt % was previously observed in peptides and small solutes (urea, formamide) and assigned to out-of-plane

dx.doi.org/10.1021/jp2074539 |*J. Phys. Chem. A* XXXX, XXX, 000–000

bending of the H-bonded solute.[11,28,66] An ~80 cm^{-1} mode was also found in the aqueous protein solutions studied through various techniques, which was assigned to protein backbone motion.[70−72] Low frequency Raman spectra of lysozyme crystals (water content 9 wt %)[64] also exhibit a mode at 83 cm^{-1}. On this basis, and on the basis of our previous studies,[11] we assign this mode to a bending of H-bonded amino acids in the protein. Even though the three proteins studied differ in their size and structure, the frequency and relative weight of the G mode is comparable. The numbers of amino acids at the same concentration are similar, for example at 10 wt % there are (6.3−6.7) × 10^{23} amino acids per liter of protein solution for BSA, lysozyme, and trypsin. Therefore, the appearance of this mode depends only on the amount of amino acid residues in the solution and not on the protein conformation.

CONCLUSIONS

Direct time domain OHD-OKE measurements on aqueous protein solutions were performed as a function of concentration. At low protein concentrations (below 5 wt %) the H-bonded structure of water is mainly preserved. Further addition of protein leads to the gradual disruption of water structure, as judged by the decrease in amplitude and frequency of the collective water−water stretching mode at 175 cm^{-1}. The picosecond relaxation times observed were associated with relaxation of H-bond network. This relaxation time was observed to increase with increasing protein concentration. A simple two-state analysis allowed us to estimate the effect of protein on water dynamics in hydration shell. In all cases water molecules in the solvation shell of the protein exhibited slower dynamics relative to bulk water. The slowest dynamics were observed for BSA, which has the most hydrophilic surface. A somewhat smaller effect was observed for the most hydrophobic protein, trypsin. These data imply that all water molecules solvating the protein surface exhibit slower relaxation than in bulk, and that hydrophilic sites influence water dynamics in their vicinity to a greater extent than hydrophobic ones. The mode observed at ~80 cm^{-1} in more concentrated protein solutions was assigned to the out-of-plane bending mode of protein units.

ACKNOWLEDGMENT

We are grateful to EPSRC for financial support of this research (EP/E010466). K.M. thanks UEA for the award of a studentship.

REFERENCES

(1) Feig, M.; Pettitt, B. M. *Biopolymers* **1998**, *48*, 199.
(2) Halle, B.; Denisov, V. P. *Biopolymers* **1998**, *48*, 210.
(3) Perticaroli, S.; Comez, L.; Paolantoni, M.; Sassi, P.; Lupi, L.; Fioretto, D.; Paciaroni, A.; Morresi, A. *J. Phys. Chem. B* **2010**, *114*, 8262.
(4) Bizzarri, A. R.; Cannistraro, S. *J. Phys. Chem. B* **2002**, *106*, 6617.
(5) Heugen, U.; Schwaab, G.; Brundermann, E.; Heyden, M.; Yu, X.; Leitner, D. M.; Havenith, M. *Proc. Natl. Acad. Sci. U. S. A.* **2006**, *103*, 12301.
(6) Shenogina, N.; Keblinski, P.; Garde, S. *J. Chem. Phys.* **2008**, *129*, 155105.
(7) Halle, B. *Philos. Trans. R. Soc London Ser. B-Biol. Sci.* **2004**, *359*, 1207.
(8) Levy, Y.; Onuchic, J. N. *Annu. Rev. Biophys. Biomol. Struct.* **2006**, *35*, 389.
(9) Rupley, J. A.; Careri, G. *Adv. Protein Chem.* **1991**, *41*, 37.
(10) Malardier-Jugroot, C.; Johnson, M. E.; Murarka, R. K.; Head-Gordon, T. *Phys. Chem. Chem. Phys.* **2008**, *10*, 4903.
(11) Mazur, K.; Heisler, I. A.; Meech, S. R. *J. Phys. Chem. B* **2010**, *114*, 10684.
(12) Born, B.; Weingartner, H.; Brundermann, E.; Havenith, M. *J. Am. Chem. Soc.* **2009**, *131*, 3752.
(13) Modig, K.; Liepinsh, E.; Otting, G.; Halle, B. *J. Am. Chem. Soc.* **2004**, *126*, 102.
(14) Qvist, J.; Persson, E.; Mattea, C.; Halle, B. *Faraday Discuss.* **2009**, *141*, 131.
(15) Paolantoni, M.; Sassi, P.; Morresi, A.; Santini, S. *J. Chem. Phys.* **2007**, 127.
(16) Nandi, N.; Bhattacharyya, K.; Bagchi, B. *Chem. Rev.* **2000**, *100*, 2013.
(17) Bizzarri, A. R.; Wang, C. X.; Chen, W. Z.; Cannistraro, S. *Chem. Phys.* **1995**, *201*, 463.
(18) Kuntz, I. D.; Kauzmann, W. *Adv. Protein Chem.* **1974**, *28*, 239.
(19) Ebbinghaus, S.; Kim, S. J.; Heyden, M.; Yu, X.; Heugen, U.; Gruebele, M.; Leitner, D. M.; Havenith, M. *Proc. Natl. Acad. Sci. U. S. A.* **2007**, *104*, 20749.
(20) Xu, J.; Plaxco, K. W.; Allen, S. J. *J. Phys. Chem. B* **2006**, *110*, 24255.
(21) Zhong, Q.; Fourkas, J. T. *J. Phys. Chem. B* **2008**, *112*, 15529.
(22) Shirota, H.; Fujisawa, T.; Fukazawa, H.; Nishikawa, K. *Bull. Chem. Soc. Jpn.* **2009**, *82*, 1347.
(23) Hunt, N. T.; Jaye, A. A.; Meech, S. R. *Phys. Chem. Chem. Phys.* **2007**, *9*, 2167.
(24) Hunt, N. T.; Jaye, A. A.; Hellman, A.; Meech, S. R. *J. Phys. Chem. B* **2004**, *108*, 100.
(25) Shirota, H.; Castner, E. W. *J. Am. Chem. Soc.* **2001**, *123*, 12877.
(26) Heisler, I. A.; Meech, S. R. *Science* **2010**, *327*, 857.
(27) Heisler, I. A.; Mazur, K.; Meech, S. R. *J. Phys. Chem. B* **2011**, *115*, 1863.
(28) Mazur, K.; Heisler, I. A.; Meech, S. R. *J. Phys. Chem. B* **2011**, *115*, 2563.
(29) Potma, E. O.; de Boeij, W. P.; Wiersma, D. A. *Biophys. J.* **2001**, *80*, 3019.
(30) Hunt, N. T.; Kattner, L.; Shanks, R. P.; Wynne, K. *J. Am. Chem. Soc.* **2007**, *129*, 3168.
(31) Winkler, K.; Lindner, J.; Vohringer, P. *Phys. Chem. Chem. Phys.* **2002**, *4*, 2144.
(32) Lotshaw, W. T.; McMorrow, D.; Thantu, N.; Melinger, J. S.; Kitchenham, R. *J. Raman Spectrosc.* **1995**, *26*, 571.
(33) Smith, N. A.; Meech, S. R. *Int. Rev. Phys. Chem.* **2002**, *21*, 75.
(34) McMorrow, D.; Lotshaw, W. T.; Kenneywallace, G. A. *IEEE J. Quantum Electron.* **1988**, *24*, 443.
(35) Torre, R.; Bartolini, P.; Righini, R. *Nature* **2004**, *428*, 296.
(36) Mizoguchi, K.; Hori, Y.; Tominaga, Y. *J. Chem. Phys.* **1992**, *97*, 1961.
(37) Ohmine, I.; Tanaka, H. *Chem. Rev.* **1993**, *93*, 2545.
(38) Hamm, P.; Garrett-Roe, S.; Perakis, F.; Rao, F. *J. Phys. Chem. B* **2011**, *115*, 6976.
(39) Lang, E. W.; Ludemann, H. D. *Angew. Chem., Int. Ed. Engl.* **1982**, *21*, 315.
(40) Murphy, W. F. *J. Chem. Phys.* **1977**, *67*, 5877.
(41) Mazzacurati, V.; Nucara, A.; Ricci, M. A.; Ruocco, G.; Signorelli, G. *J. Chem. Phys.* **1990**, *93*, 7767.
(42) Marti, J.; Padro, J. A.; Guardia, E. *J. Chem. Phys.* **1996**, *105*, 639.
(43) Ohmine, I.; Saito, S. *Acc. Chem. Res.* **1999**, *32*, 741.
(44) Castner, E. W.; Chang, Y. J.; Chu, Y. C.; Walrafen, G. E. *J. Chem. Phys.* **1995**, *102*, 653.
(45) Laage, D.; Hynes, J. T. *Science* **2006**, *311*, 832.
(46) James, T. L.; Matson, G. B.; Kuntz, I. D. *J. Am. Chem. Soc.* **1978**, *100*, 3590.
(47) Lee, B. *Proc. Natl. Acad. Sci. U. S. A.* **1983**, *80*, 622.
(48) Marchi, M.; Sterpone, F.; Ceccarelli, M. *J. Am. Chem. Soc.* **2002**, *124*, 6787.
(49) Rejoumichel, A.; Henry, F.; Devillardi, M.; Delmotte, M. *Phys. Med. Biol.* **1985**, *30*, 831.

(50) Lerbret, A.; Affouard, F.; Bordat, P.; Hedoux, A.; Guinet, Y.; Descamps, M. *J. Chem. Phys.* **2009**, 131.
(51) Yokoyama, K.; Kamei, T.; Minami, H.; Suzuki, M. *J. Phys. Chem. B* **2001**, *105*, 12622.
(52) Qvist, J.; Halle, B. *J. Am. Chem. Soc.* **2008**, *130*, 10345.
(53) Mahn, A.; Asenjo, J. A. *Biotechnol. Adv.* **2005**, *23*, 359.
(54) Eriksson, K. O.; Naidu, A. S.; Kilar, F.; Wadstrom, T.; Hjerten, S. *APMIS* **1989**, *97*, 1081.
(55) Kato, A.; Nakai, S. *Biochim. Biophys. Acta* **1980**, *624*, 13.
(56) Moon, Y. U.; Curtis, R. A.; Anderson, C. O.; Blanch, H. W.; Prausnitz, J. M. *J. Solution Chem.* **2000**, *29*, 699.
(57) Lee, B.; Richards, F. M. *J. Mol. Biol.* **1971**, *55*, 379.
(58) de Morais, L. C.; Bernardes, R.; Assis, O. *World J. Microbiol. Biotechnol.* **2009**, *25*, 123.
(59) Rezus, Y. L. A.; Bakker, H. J. *Phys. Rev. Lett.* **2007**, *99*, 148301.
(60) Heyden, M.; Havenith, M. *Methods* **2010**, *52*, 74.
(61) Stirnemann, G.; Hynes, J. T.; Laage, D. *J. Phys. Chem. B* **2010**, *114*, 3052.
(62) Russo, D.; Hura, G.; Head-Gordon, T. *Biophys. J.* **2004**, *86*, 1852.
(63) Nakayama, T. *Phys. Rev. Lett.* **1998**, *80*, 1244.
(64) Urabe, H.; Sugawara, Y.; Ataka, M.; Rupprecht, A. *Biophys. J.* **1998**, *74*, 1533.
(65) Bucaro, J. A.; Litovitz, T. A. *J. Chem. Phys.* **1971**, *54*, 3846.
(66) Nielsen, O. F.; Lund, P. A.; Praestgaard, E. *J. Chem. Phys.* **1982**, *77*, 3878.
(67) Chang, Y. J.; Castner, E. W. *J. Chem. Phys.* **1993**, *99*, 113.
(68) Hunt, N. T.; Turner, A. R.; Tanaka, H.; Wynne, K. *J. Phys. Chem. B* **2007**, *111*, 9634.
(69) Laage, D.; Stirnemann, G.; Hynes, J. T. *J. Phys. Chem.* **2009**, *113*, 2428.
(70) Giraud, G.; Karolin, J.; Wynne, K. *Biophys. J.* **2003**, *85*, 1903.
(71) Colaianni, S. E. M.; Nielsen, O. F. *J. Mol. Struct.* **1995**, *347*, 267.
(72) Eaves, J. D.; Fecko, C. J.; Stevens, A. L.; Peng, P.; Tokmakoff, A. *Chem. Phys. Lett.* **2003**, *376*, 20.